Light propagation in dry and wet softwood

Alwin Kienle[1], Cosimo D'Andrea[2], Florian Foschum[1], Paola Taroni[2], and Antonio Pifferi[2]

[1] *Institut für Lasertechnologien in der Medizin und Meßtechnik, Helmholtzstr.12, D-89081 Ulm, Germany*

[2] *CNR-INFM and CNR-IFN, Dipartimento di Fisica, Politecnico di Milano, Piazza Leonardo da Vinci 32, 20133 Milano, Italy*

alwin.kienle@ilm.uni-ulm.de

Abstract: Light propagation in dry and wet softwood (silver fir) was investigated experimentally and theoretically. The spatially and time resolved reflectance from softwood was measured. Light propagation was modeled with Monte Carlo simulations considering the microstructure of softwood. By comparing the spatially resolved reflectance we found that all characteristics of the experimentally obtained iso-intensity contour lines were recovered by the theory. In addition, the reduced scattering and the absorption coefficients were determined in the time domain by fitting a solution of the diffusion equation to Monte Carlo simulations and to measurements. Good qualitative agreement was obtained between the experimentally and theoretically derived optical properties.

OCIS codes: (290.4210) Multiple scattering; (290.1990) Diffusion; (170.7050) Turbid media.

References and links

1. J. M. Dinwoodie, "Timber: Its Nature and Behaviour," Taylor & Francis (2000).
2. J. Zhou, J. Shen: "Improved Phase Demodulation for Grain Orientation Measurement," Opt. Lasers Eng. **45,** 160–169 (2007).
3. S.P. Simonaho, J. Palviainen, Y. Tolonen, R. Silvennoinen: "Determination of Wood Grain Direction from Laser Light Scattering Pattern," Opt. Lasers Eng. **41,** 95–103 (2002).
4. S. Tsuchikawa: "A Review of Recent Near Infrared Research for Wood and Paper," Appl. Spectr. Rev. **42**, 43–71 (2007).
5. S.S. Kelley, T.G. Rials, R. Snell, L.H. Groom, A. Sluiter: "Use of Near Infrared Spectroscopy to Measure the Chemical and Mechanical Properties of Solid Wood," Wood Sci. Technolo. **38**, 257–276 (2004).
6. S.P. Simonaho, R. Silvennoinen: "Light Diffraction from Wood Tissue," Opt. Rev. **11**, 308–311 (2004).
7. K. Saarinen, K. Muinonen: "Light Scattering by Wood Fibres," Appl. Opt. **40**, 5064–5077 (2001).
8. M. Andersson, L. Persson, M. Sjöholm, S. Svanberg: "Spectroscopic Studies of Wood-Drying Processus," Opt. Express **14**, 3641–3653 (2006).
9. S. Tsuchikawa, S. Tsutsumi: Application of "Time-of-Flight Near-Infrared Spectroscopy to Wood with Anisotropic Cellular Structure," Appl. Spectrosc. **56**, 869–876 (2002).
10. S.R. Marschner, S.H. Westin A. Arbree, J.T. Moon: "Measuring and Modeling the Appearance of Finished Wood," International Conference on Computer Graphics and Interactive Techniques, ACM SIGGRAPH, 727–734 (2005).
11. A. Kienle, F.K. Forster, R. Hibst: "Anisotropy of Light Propagation in Biological Tissue," Opt. Lett. **29**, 2617–2619 (2004).
12. A. Kienle, C. Wetzel, A. Bassi, D. Comelli, P. Taroni, A. Pifferi: "Determination of the Optical Properties of Anisotropic Biological Media using an Isotropic Model," J. Biomed. Opt. **12**, 014026 (2007).
13. A. Ishimaru: Wave Propagation and Scattering in Random Media, Academic Press, New York (1978).

#93808 - $15.00 USD Received 13 Mar 2008; revised 28 Apr 2008; accepted 9 Jun 2008; published 20 Jul 2008

14. I.D. Donato, P. Agozzino: "Composti polimerici per il consolidamento di legni degradati," Science and Technology for Cultural Heritage **13**, 71 (2004).
15. H.A. Yousif, E. Boutros: "A FORTRAN Code for the Scattering of EM Plane Waves by an Infinitely Long Cylinder at Oblique Incidence," Comput. Phys. Commun. **69**, 406–414 (1992).
16. C.F. Bohren and D.R. Huffman: Absorption and Scattering of Light by Small Particles, John Wiley & Sons, New York, USA (1983).
17. C. D'Andrea, A. Farina, D. Comelli, A. Pifferi, P. Taroni, G. Valentini, R. Cubeddu, L. Zoia, M. Orlandi, A. Kienle: "Time-Resolved Optical Spectroscopy of Wood," Appl. Spectrosc. **62**, 569–574 (2008).
18. M.S. Patterson, B. Chance, B.C. Wilson: "Time Resolved Reflectance and Transmittance for the Noninvasive Measurement of Tissue Optical Properties," Appl. Opt. **28**, 2331–2336 (1989).
19. A. Kienle: "Anisotropic Light Diffusion: An Oxymoron?," Phys. Rev. Lett. **98,** 218104 (2007).
20. A. Kienle, L. Lilge, M.S. Patterson, R. Hibst, R. Steiner, B.C. Wilson: "Spatially-Resolved Absolute Diffuse Reflectance Measurements for Non-Invasive Determination of the Optical Scattering and Absorption Coefficients of Biological Tissue," Appl. Opt. **35**, 2304–2314 (1996).
21. A. Pifferi, A. Torricelli, P. Taroni, D. Comelli, A. Bassi, R. Cubeddu: "Fully Automated Time Domain Spectrometer for the Absorption and Scattering Characterization of Diffusive Media," Rev. Sci. Instrum. **78,** 053103 (2007).
22. S.P. Simonaho, Y. Tolonen, J. Rouvinen, R. Silvennoinen: "Laser Light Scattering from Wood Samples Soaked in Water or in Benzyl Benzoate," Optik **114**, 445–448 (2003).

1. Introduction

Knowledge of light propagation in wood is important for industrial applications as well as for understanding the optical appearance of wood. For a correct description of the optics of wood the aligned microstructure, which causes the anisotropic optical properties of wood, has to be considered.

Wood is a complex material [1]. It shows structural variations on different scales which reveal the three main functions that trunk has to fulfill: i) to support the crown; ii) to conduct mineral solution from the roots to the crown; iii) to store nutritious material. At a microscopic level, four basic cell types constitute the wood: parenchyma, tracheids, fibres and vessels (or pores). In particular, according to cellular structure, wood types are usually classified into two main classes: softwood (coniferous wood) and hardwood. Softwood presents a simpler structure compared with hardwood and it is composed of only two types of cell: tracheids and parenchyma. The first are more numerous (about 90%) and accomplish the functions of support and conduction. Tracheids ($2-4$ mm long and $20-40\,\mu$m wide) are lined up vertically along the tree. On the contrary parenchyma cells are mostly located in bands (called rays) belonging to radial planes and accomplishing food storage. The high anisotropy of wood can be explained with the different distributions of cells along the three axes.

In literature, the anisotropic light pattern obtained by measurement of the spatially resolved reflectance from wood, which was illuminated by a point source, has been studied to determine the grain orientation [2, 3]. Furthermore, near infrared (NIR) spectroscopy has been applied to correlate NIR spectra to chemical and physical properties of wood [4, 5]. Due to the high scattering in wood and its anisotropic optical properties, the NIR spectra depend strongly on the light propagation and, thus, on the measurement position relative to the wood fiber direction.

Studies were performed to investigate the scattering by wood fibers [6, 7]. A strong anisotropic scattering behavior was found. Recently, the drying process of wood was measured via wavelength-modulation diode laser spectroscopy [8].

Time resolved measurements were also performed on wood samples to study its optical characteristics [9]. In addition, the appearance of wood was modeled for realistic computer animation [10].

Although knowledge of wood optics is important for all these applications, no complete model has been proposed, with which it is possible to describe the light propagation in wood on the microscopic and macroscopic scale. Marschner *et al.* [10] recognized the importance of

#93808 - $15.00 USD Received 13 Mar 2008; revised 28 Apr 2008; accepted 9 Jun 2008; published 20 Jul 2008

considering the three-dimensional scattering characteristics of wood fibers, but they introduced several approximations. For example, realistic phase functions for the fibers were not applied and also multi-scattering was not explicitly considered. These approximations were feasible because they regarded only the angularly resolved reflectance and not the spatially and time resolved reflectance.

In this study we investigated the light propagation in softwood considering its microstructure. We assumed that the tracheids can be described by long cylinders, which are the main cause for the anisotropic light propagation. In addition, we assumed that the other scatterers in wood, for example the components of the cell walls (e.g. cellulose, lignin), the pits or the parenchyma can collectively be described by scatterers which have isotropic optical properties. Using this microstructural model for wood we applied Monte Carlo simulations to solve the transport equation numerically. In the steady-state domain we compared the simulated results for the spatially resolved reflectance with measurements using a CCD-Camera. In the time domain we determined the absorption and the reduced scattering coefficients of wood fitting a solution of the time resolved diffusion equation to Monte Carlo simulations and to experimental data. Recently, we showed that with a similar model the main features of the light propagation in arteries and tendon could be successfully explained [11, 12].

2. Theory

We used two theoretical models to describe light propagation in wood. Transport theory was applied to model the light propagation considering the microstructure of wood. The transport equation was solved using the Monte Carlo method. On the other hand the diffusion theory, which is an approximation of the transport theory, was used to determine the optical properties of wood [13]. We employed the isotropic diffusion theory, which does not account for the anisotropic optical coefficients found in wood. However, we recently showed with time resolved reflectance measurements that it is possible to derive the absorption coefficient of turbid media having anisotropic scattering properties within an error of $\approx 10\%$ using the solution of the isotropic diffusion theory [12].

2.1. Monte Carlo simulations

A description of our Monte Carlo code was presented elsewhere [11]. Here we mention only the specific features of the code used in this study.

Softwood mainly consists of elongated cells, the tracheids, lying approximately parallel to the stem direction. The average diameter of these hollow fibers is $d \approx 30\,\mu$m [9]. The wall thickness of the cells is in the range of a few micrometers. Figure 1 shows the geometry of the microstructure of softwood used in our simulations.

We assumed that the tracheids are infinitely long parallel cylinders in direction of the x-axis having a diameter of $d = 30\,\mu$m. For the minimal wall thickness we used $3\,\mu$m. Thus, it follows that about 35% of the volume is wood substance and 65% is filled with air for dry wood and with water for wet wood. These values are close to porosity measurements performed on silver fir (abies alba) wood by means of a pycnometer [14], leading to a porosity of 70%. The refractive index of the wood substance was assumed to be $n = 1.55$ [7] and that of air and water $n = 1.0$ and $n = 1.33$, respectively. Thus, we obtained an average index of refraction for dry wood of $n_{dry} = 1.19$ and for wet wood of $n_{wet} = 1.41$ using the arithmetical mean weighted by the volume percentage of wood substance and air or water. In order to describe the scattering of all other structures in wood we assumed isotropic optical properties (i.e. independent of the incident direction) characterized with a reduced scattering coefficient, $\mu'_{s,iso}$, and an anisotropy factor, which equaled $g = 0.9$ using a Henyey-Greenstein phase function. The use of alternative phase functions do not change significantly the presented results.

#93808 - $15.00 USD Received 13 Mar 2008; revised 28 Apr 2008; accepted 9 Jun 2008; published 20 Jul 2008

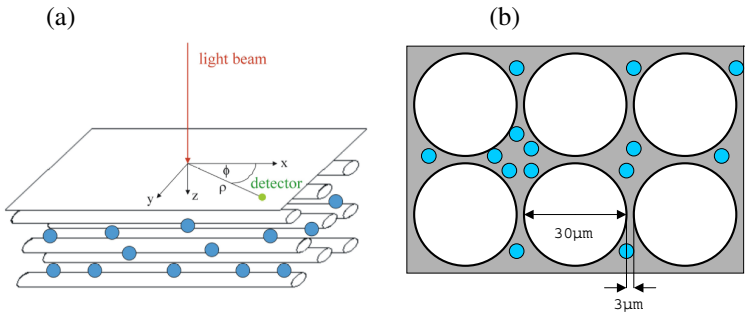

Fig. 1. Scheme of the geometrical arrangement of the cylindrical scatterers and the scatterers having isotropic optical properties. (a) Three dimensional view; (b) cross section in the y-z-plane.

The scattering by the tracheids was calculated using the solution of the Maxwell equations for a plane wave, which is incident onto an infinitely long cylinder [15]. The angle between the direction of the photon and that of the cylinders is termed ξ. The light scattered by an infinitely long cylinder is restricted to certain scattering directions. The calculations show that the photons are scattered in a cone with the cylinder as the axis of the cone having a half angle ξ [16]. The probability for light scattering around the scattering cone is described by the corresponding phase function and depends strongly on ξ. We used the phase functions for the scattering by the cylinders for ξ-values between 0° and 90° in steps of $\Delta\xi = 1^\circ$ in the Monte Carlo simulations. For the solution of the Maxwell equations the refractive index inside the cylinder was set to 1.0 for dry wood and to 1.33 for wet wood, whereas the refractive index outside the cylinder was always 1.55.

The number density of the cylinders in our model was $c_a = 918\,\mathrm{mm}^{-2}$, compare Fig. 1. The scattering coefficient μ_s of the cylinders was computed with

$$\mu_s(\xi) = Q_{sca}(\xi)\, d\, c_a\,, \tag{1}$$

where Q_{sca} is the scattering efficiency of a single cylinder, which depends on the incident angle ξ and was also calculated with the solution of the Maxwell equation [15]. Thus, in addition to the phase function, also the scattering coefficient depends on the propagation direction of the photon relative to the cylinder axis. We assumed independent scattering of the cylinders.

To get an idea of the scattering power of the tracheids in our model, we calculated the reduced scattering coefficient for an isotropic distribution of the cylinders considering the ξ-dependent scattering coefficient and phase function. In this case it is possible to calculate an effective phase function which is independent of the incident angle. For wet and dry wood we obtained an anisotropy factor of $g = 0.959$ and $g = 0.850$, a scattering coefficient of $\mu_s = 43.8\,\mathrm{mm}^{-1}$ and $\mu_s = 44.6\,\mathrm{mm}^{-1}$, and, thus, a reduced scattering coefficient of $\mu_s' = \mu_s(1-g) = 1.79\,\mathrm{mm}^{-1}$ and $\mu_s' = 6.68\,\mathrm{mm}^{-1}$, respectively. Therefore, the effective scattering due to the tracheids (characterized by μ_s') is almost 4 times higher for dry wood as compared to wet wood.

For the Monte Carlo simulations the geometry of the softwood sample was assumed to be semi-infinite. The photons were incident in z-direction and, thus, perpendicular to the cylinder direction, compare Fig. 1. After each interaction the scattering coefficient due to the cylinders was calculated considering the actual ξ-value and was compared to the scattering coefficient due to the isotropic scattering, $\mu_{s,iso}$. Using these values and a random number it was decided, if the photon was scattered by the cylinders or by the scatterers having isotropic optical properties [11].

#93808 - $15.00 USD Received 13 Mar 2008; revised 28 Apr 2008; accepted 9 Jun 2008; published 20 Jul 2008

Simulations were performed to obtain the spatially resolved and time resolved reflectance. A gaussian beam profile with a radius of 0.25 mm was used to characterize the incident beam. The absorption coefficient was set to $\mu_a = 0.005\,\mathrm{mm}^{-1}$ both for wet and dry wood. This value was obtained by recent time resolved measurements on dry and wet wood of the same tree at $\lambda = 800\,\mathrm{nm}$ [17].

2.2. *Diffusion theory*

A solution of the isotropic diffusion theory for a semi-infinite medium using extrapolated boundary conditions was employed to derive the reduced scattering and absorption coefficients in the time domain [18]. Recently, we showed that the use of the anisotropic diffusion equation has no advantage for this application [19]. The refractive indices of dry and wet wood were set to the same values which were applied in the Monte Carlo simulations ($n_{dry} = 1.19$, $n_{wet} = 1.41$).

The absorption and the reduced scattering coefficients were derived with a non-linear regression algorithm using the solution of the diffusion equation in the time domain [12]. For the non-linear regression to the Monte Carlo data the start time of the fitting range was the peak of the time resolved reflectance and the end time was the time at which the reflectance was about two orders of magnitude smaller. The weights used in the non-linear regression were calculated using Poisson statistics.

Analogous to the fitting of the Monte Carlo data, time resolved experimental curves were fitted with the solution of the time dependent diffusion equation [18]. The theoretical curves were convolved with the instrumental response function and normalized to the area of the experimental curve. The fitting procedure was limited to the data which have a number of counts higher than 80% of the peak on the rising part of the curve and higher than 1% on the tail. In general, the fitted optical properties had mean differences smaller than 10% when different start and end times were used.

3. Materials and methods

3.1. *Spatially resolved reflectance*

The measurement of the spatially resolved reflectance was described in detail elsewhere [20]. Briefly, the wood sample was illuminated almost perpendicularly (about 10°) to the wood surface at $x = y = 0\,\mathrm{mm}$ in z-direction using a laser diode at $\lambda = 808\,\mathrm{nm}$, compare Fig. 1. The remitted light was measured spatially resolved by imaging the wood surface onto a 16-bit CCD-Camera. The geometry of the wood sample was a rectangular parallel-epiped with dimensions of $\approx 3 \times 5 \times 5\,\mathrm{cm}^3$. This geometry can be considered as semi-infinite for the spatially resolved reflectance measurements performed in this study. The tracheids were aligned in x-direction, so that they had an angle of $\xi = 90°$ relative to the incident beam. No polarizers were used in the experiments. In order to form a circular beam profile, the light of the laser diode was coupled into an optical fiber. The distal end of the fiber was imaged onto the sample surface. The radius of the beam at the wood surface was 0.25 mm.

As an example of softwood a silver fir sample was chosen. The sample is a piece of wood, which has followed a standard seasoning procedure for woodworking purposes. First, the wood sample was placed in water for about 2 weeks until the weight did only increase very slowly. The mass of the wet sample was $m = 60.3\,\mathrm{g}$. Then, the wood sample was placed in air and reflectance measurements were performed at different time intervals. Measurements were continued for about one week until the weight did not decrease anymore. The mass of dry wood was $m = 30.7\,\mathrm{g}$. However, after several hours in air no changes in the reflectance measurements from the sample were recorded. Obviously, the wet wood sample was drying from the borders

#93808 - $15.00 USD Received 13 Mar 2008; revised 28 Apr 2008; accepted 9 Jun 2008; published 20 Jul 2008

in direction to the center of the sample. After several hours in air the wood sample was dry until a certain depth, so that almost all of the remitted photons measured in the spatially resolved reflectance experiments were propagating in the dry region.

3.2. Time resolved reflectance

Time resolved measurements were carried out on a sample of larger dimensions ($\approx 8 \times 5 \times 5\,\mathrm{cm}^3$) obtained from the same piece of wood. A time resolved diffuse optical spectroscopy set-up was used for the measurement of the optical parameters. A detailed description of the set-up can be found in [21]. An active mode-locking Ti:Sapphire laser emits picosecond pulses at a repetition rate of about 80 MHz at a selected wavelength over the spectral range 700-1040 nm. Two optical fibers were placed on the same side of the sample (reflectance geometry) at a known distance (interfiber distance). The first fiber delivered the light pulse on the wood sample, while the second one collected the diffused light exiting the sample and was coupled to a double microchannel plate photomultiplier tube.

The two fibers were inserted into a fiber holder made of a black teflon block with holes at steps of 5 mm drilled on two orthogonal lines so to probe the wood along directions parallel and perpendicular to the fibers. In order to avoid direct coupling of the illuminating light into the collecting fiber, the surface of the Teflon block in contact with the sample was covered with a velvet foil with tiny holes in correspondence to the fiber positions. Further, the fiber holder was pressed against the wood sample to assure a perfect shielding of both fibers.

Time resolved curves were obtained by means of a time-correlated single photon counting (TCSPC) PC board. By changing the wavelength of the injected light it is possible to acquire the time resolved curves over the 700-1040 nm spectral range. In this study measurements at 800 nm are presented. Finally, the instrumental response function (IRF) was measured by delivering a small fraction of the laser light directly to the detector. The IRF resulted to be less than 180 ps (FWHM) over the entire spectral range.

Measurements were carried out on dry and wet woods, respectively. The wet sample remained immersed in water for 8 weeks reaching a mass of 260 g (the mass of dry sample was 88 g). A weekly control of the weight was performed, revealing that after that time no further increase of the weight was present. Both samples were measured in two different geometries: in the first case the line connecting the tips of the injection/detection fibers was aligned parallel to x-direction (parallel to tracheids) while in the second case it was perpendicular to the tracheids direction.

4. Results

4.1. Spatially resolved reflectance

Figure 2(a) and (b) show the iso-intensity contour lines of the experimental spatially resolved reflectance from wet and dry wood, respectively, which were illuminated with a laser diode at $\lambda = 808$ nm. The measurements of the wet sample were performed about 1 min after the wood was taken from the water basin into air. The experiment on the dry sample has been carried out after the sample was in air for 1341 min.

The iso-intensity contour lines of the dry and wet sample exhibit elliptical shapes elongated in x-direction (the direction of the tracheids) at large distances from the incident source. At medium distances the patterns are rhombic, and at small distances from the source the iso-intensity contour-lines are again elongated, but here in y-direction. At very small distances the contour lines are circular due to the circular incident laser beam. In general, the reflectance decreases much faster with increasing distances for the dry wood as compared to the wet wood. The elliptical pattern elongated in y-direction at small distances is not visible in the measurement on the dry sample due to the finite diameter of the incident laser beam and the faster

#93808 - $15.00 USD Received 13 Mar 2008; revised 28 Apr 2008; accepted 9 Jun 2008; published 20 Jul 2008

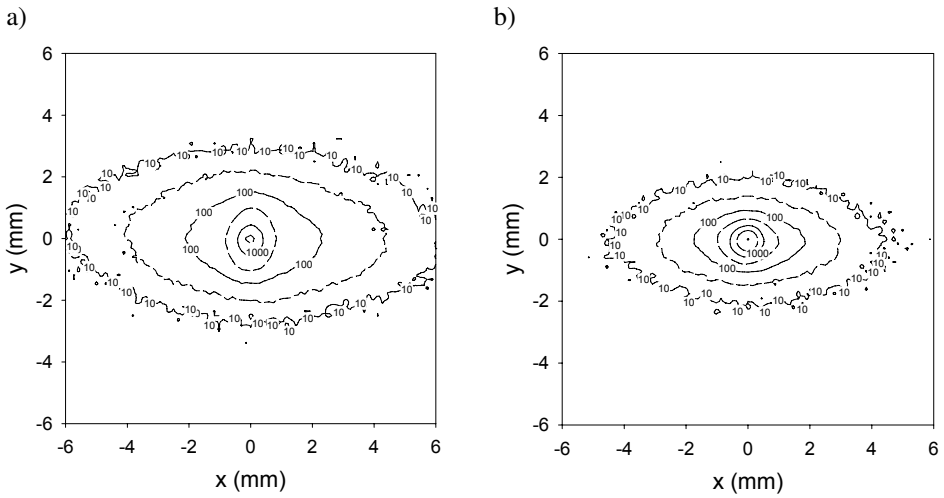

Fig. 2. Iso-intensity contour lines of the experimental spatially resolved reflectance $R(x,y)$ from (a) the wet and (b) the dry wood sample. The numbers are given in counts of the CCD-Camera pixels.

decrease of the spatially resolved reflectance with increasing distance. Another feature is that the ellipticity is more pronounced in the measurements of the dry wood as compared to the wet wood. Similar experimental results have been found by Simonaho et al. [22], however, their explanation was very different to ours, see discussion chapter.

The results obtained from the Monte Carlo simulations are shown in Fig. 3. The numerical values of the optical properties used in the calculations are given in the theory chapter with the exception of $\mu'_{s,iso}$. As we did not know $\mu'_{s,iso}$ either for wet or for dry wood, we performed a set of Monte Carlo simulations for different $\mu'_{s,iso}$-values between $0.2\,\mathrm{mm}^{-1}$ and $2\,\mathrm{mm}^{-1}$ keeping all other optical properties constant. We found that with $\mu'_{s,iso} = 1.5\,\mathrm{mm}^{-1}$ and $\mu'_{s,iso} = 0.8\,\mathrm{mm}^{-1}$ for dry and wet wood, respectively, the smallest differences to the experiments were obtained.

All the characteristics found in the experimental reflectance can also be seen in the results of the Monte Carlo simulations. In addition, the elliptical iso-intensity contour lines at small distances, which could not be observed for the dry wood sample due to the finite beam radius, can now be easily observed by decreasing the beam radius in the simulations (Fig. not shown). With the simulated results we are able to understand all features of the reflectance pattern. When the incident photons are scattered the first time by the cylinders the angle between the cylinders and the photon direction is $\xi = 90^\circ$. Thus, the photons are scattered in the y-z-plane due to the characteristics of the scattering of a plane wave by a long cylinder [16]. Therefore, at small distances the iso-intensity contour lines are elongated in y-direction. If there were only cylindrical scatterers, all photons would be remitted close to the y-axis. However, due to the scatterers that have isotropic optical properties the photons can obtain arbitrary directions in the scattering medium. After many scattering interactions the photons will propagate further in the x-direction, because the scattering coefficient along the cylinders is much smaller than that perpendicular to the cylinders [12]. Therefore, at large distances we obtain iso-intensity lines that are elongated in x-direction [12]. At medium distances the transition of the two cases described above becomes manifested in rhombic iso-intensity contour lines. Quantitatively however, the experimental and theoretical data exhibit differences, which are argued in the discussion chap-

#93808 - $15.00 USD Received 13 Mar 2008; revised 28 Apr 2008; accepted 9 Jun 2008; published 20 Jul 2008

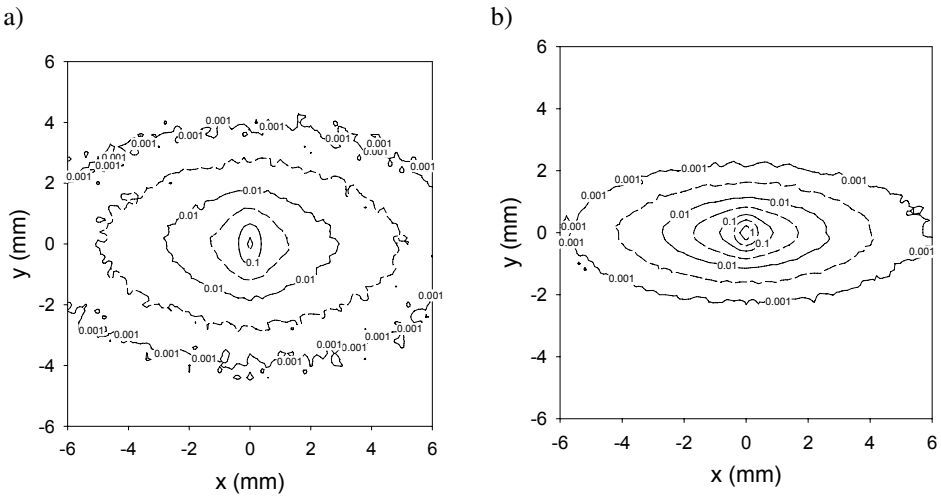

Fig. 3. Iso-intensity contour lines of the spatially resolved reflectance $R(x,y)$ from a) the wet and b) the dry wood sample calculated with the Monte Carlo method. The numbers indicate the probability that an incident photon is remitted per mm^{-2}.

ter.

In order to compare the experimental and theoretical data for the wet and dry wood more quantitatively, Fig. 4 shows the spatially resolved reflectance $R(x,y)$ of Fig. 2 and Fig. 3 along the x-axis ($R(x) = R(x, y = 0)$) and along the y-axis ($R(y) = R(x = 0, y)$). For this comparison we multiplied all experimental curves by the same factor to convert the pixel counts of the CCD-Camera measurements into the reflectance calculated by the Monte Carlo method. In Fig. 4 the good qualitative agreement between experiment and theory can be seen more precisely than in the contour plots. At small distances the reflectance of the theoretical data is smaller than that of the corresponding experiments. This is caused by the incident light that is reflected from the rough wood surface. In the Monte Carlo simulation we did not consider the reflected light due to the unknown topology of the wood surface. Relatively large differences can be seen in $R(y)$ for dry wood at large distances. This is, at least partly, due to the point spread function of the CCD-Camera system.

Fig. 5 shows reflectance measurements along the x- and y-direction, $R(x)$ and $R(y)$, during the drying process at different times between 1 min and 1341 min after the wood sample was put in air.

It can be observed how $R(x)$ and $R(y)$ decrease for large distances and increase for small distances from the incident source. After a drying time of about 400 min there is almost no change in the reflectance curves indicating that the wood was dry at a superficial layer in which most of the detected photons propagated.

4.2. Time resolved reflectance

Monte Carlo simulations were performed in the time domain to obtain the time resolved reflectance using the same model and optical properties as for the calculation of the spatially resolved reflectance. Figure 6 shows, as an example, $R(t, x = 4.5\,\mathrm{mm}, y = 0)$ and $R(t, x = 0, y = 4.5\,\mathrm{mm})$ from the wet and the dry wood sample.

Large differences of the reflectance can be observed both between the data on the x- and y-axes and the simulations for wet and dry wood. By time integration of the curves in Fig. 6 the values of the spatially resolved reflectance shown in Fig. 3 can be obtained.

#93808 - $15.00 USD Received 13 Mar 2008; revised 28 Apr 2008; accepted 9 Jun 2008; published 20 Jul 2008

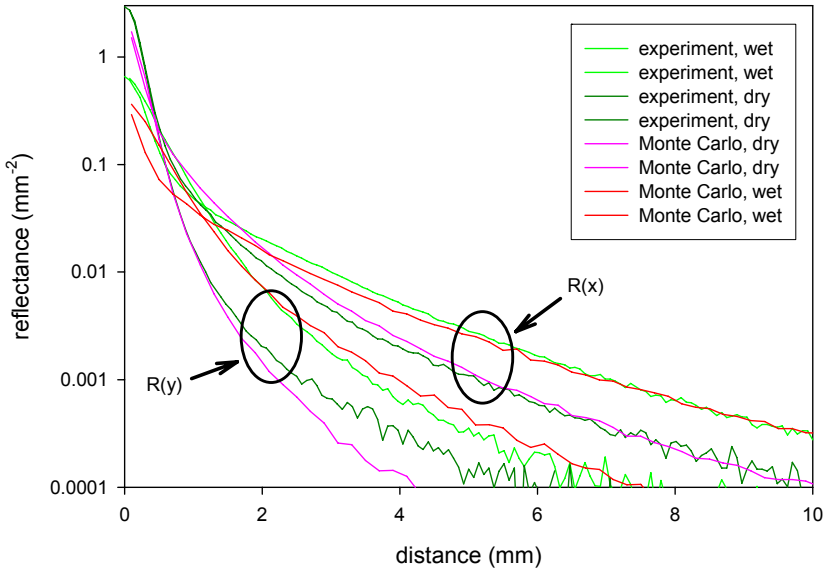

Fig. 4. $R(x)$ and $R(y)$ of dry and wet wood obtained from the experimental and simulated data shown in Fig. 2 and Fig. 3.

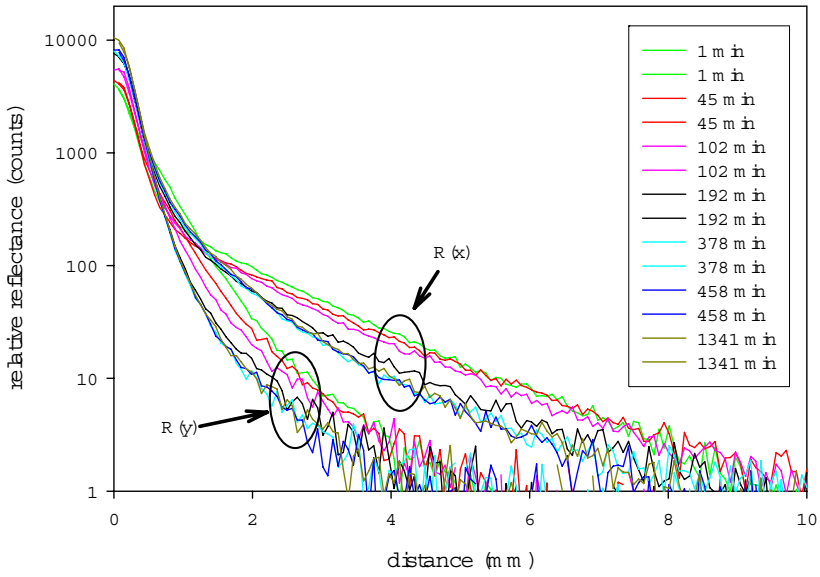

Fig. 5. Spatially resolved reflectance (in pixel counts) along the x- and y-direction during the drying process of the wood sample.

#93808 - $15.00 USD Received 13 Mar 2008; revised 28 Apr 2008; accepted 9 Jun 2008; published 20 Jul 2008

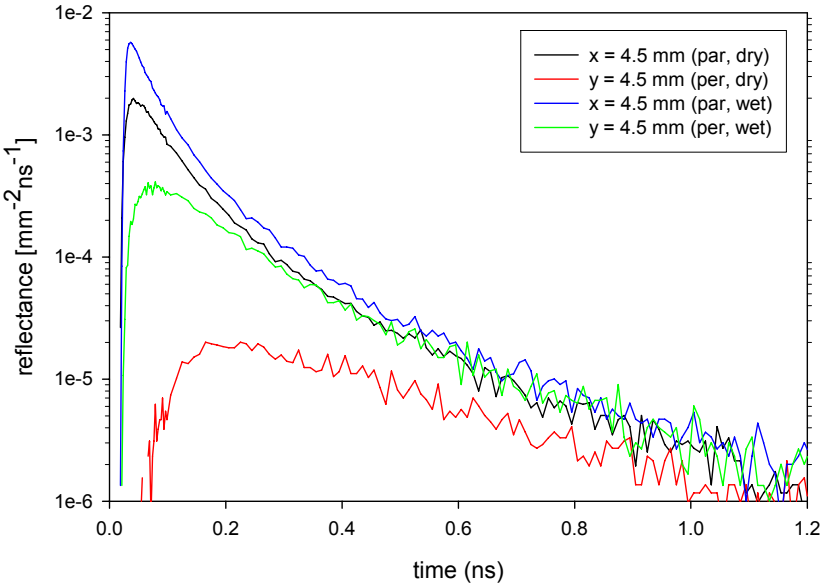

Fig. 6. Time resolved reflectance $R(t)$ from wet and dry wood at a distance of 4.5 mm ($x = 4.5$ mm, $y = 0$ mm or $x = 0$ mm, $y = 4.5$ mm) from the incident source calculated by the Monte Carlo method.

We fitted the time resolved reflectance with the solution of the diffusion equation at different distances from the source on the x- and the y-axes. The distance range used in the fit (between 5 and 15 mm) was chosen as a compromise between the validity of the diffusion equation, which affords large distances, and the better statistics of the Monte Carlo simulations for small distances. For the absorption coefficient we got $\mu_a = 0.005\,\mathrm{mm}^{-1} \pm 0.001\,\mathrm{mm}^{-1}$ for both the measurements parallel and perpendicular to the tracheids' direction. As we used an absorption coefficient of $\mu_a = 0.005\,\mathrm{mm}^{-1}$ in the Monte Carlo simulations, this result confirms that it is possible to recover the absorption coefficient of a turbid medium having anisotropic optical properties using the time resolved isotropic diffusion equation [12]. For the reduced scattering coefficient we obtained for the dry wood $\mu_s' = 1.7\,\mathrm{mm}^{-1} \pm 0.1\,\mathrm{mm}^{-1}$ parallel to the tracheids and $\mu_s' = 10\,\mathrm{mm}^{-1} \pm 1\,\mathrm{mm}^{-1}$ perpendicular to the tracheids. The corresponding values for the wet wood were $\mu_s' = 0.8\,\mathrm{mm}^{-1} \pm 0.1\,\mathrm{mm}^{-1}$ parallel to the tracheids and $\mu_s' = 2.4\,\mathrm{mm}^{-1} \pm 0.3\,\mathrm{mm}^{-1}$ perpendicular to the tracheids, see Tab. 1.

Tab. 1: Reduced scattering coefficients derived from non-linear regression on Monte Carlo simulations and experiments for measurements parallel (par) or perpendicular (per) to the tracheids' direction on dry and wet wood.

	$\mu'_{s\,par\,dry}[\mathrm{mm}^{-1}]$	$\mu'_{s\,per\,dry}[\mathrm{mm}^{-1}]$	$\mu'_{s\,par\,wet}[\mathrm{mm}^{-1}]$	$\mu'_{s\,per\,wet}[\mathrm{mm}^{-1}]$
Monte Carlo	1.7	10	0.8	2.4
Experiment	1.8	13	0.6	2.0

An example of the experimental data is shown in Fig. 7. The time resolved reflectance measurement (small diamonds) for the wet wood taken along the fiber directions is fitted with the convolution (solid line) of the theoretical model with the system response (dashed line).

Analogous to the Monte Carlo simulations, experimental time resolved reflectance curves at

#93808 - $15.00 USD Received 13 Mar 2008; revised 28 Apr 2008; accepted 9 Jun 2008; published 20 Jul 2008

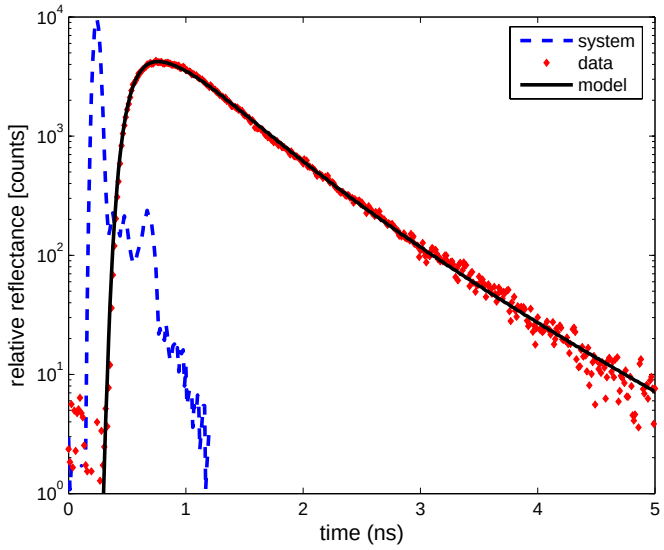

Fig. 7. Fit of the time resolved reflectance measurements (small diamonds) for the wet wood taken along the fiber directions with the convolution (solid line) of the theoretical model with the system response (dashed line). The interfiber distance was 25 mm.

800 nm were fitted with the solution of the diffusion equation. Hereafter the calculated optical parameters for dry/wet woods in the two geometrical configurations are reported. The four different measurements show huge variation of the intensity of the diffused signal, hence different distances between injection and detection fibers were chosen. In particular, with the dry sample the interfiber distance was 20 mm and 10 mm for the measurements parallel and perpendicular to tracheids' direction, respectively. The interfiber distance, with the wet sample, was 25 mm and 15 mm for the experiments parallel and perpendicular to tracheids' direction, respectively. In all cases we assumed to be in the range of validity of the diffusion equation. First we analyzed dry wood obtaining the following absorption coefficients, $\mu_a = 0.0048\,\mathrm{mm}^{-1}$ and $\mu_a = 0.0042\,\mathrm{mm}^{-1}$ for the measurement parallel and perpendicular to the tracheids' direction, respectively. For the reduced scattering coefficient we got $\mu_s' = 1.8\,\mathrm{mm}^{-1}$ and $\mu_s' = 13\,\mathrm{mm}^{-1}$ for the direction parallel and perpendicular, respectively. In the case of wet wood we obtained similar values of the absorption coefficient as for the dry sample: $\mu_a = 0.0045\,\mathrm{mm}^{-1}$ (parallel to tracheids' direction) and $\mu_a = 0.0038\,\mathrm{mm}^{-1}$ (perpendicular to tracheids' direction). For what concern the reduced scattering coefficient we got a strong reduction, $\mu_s' = 0.6\,\mathrm{mm}^{-1}$ and $\mu_s' = 2.0\,\mathrm{mm}^{-1}$ for the direction parallel and perpendicular, respectively, see Tab. 1.

5. Discussion

Spatially and time resolved reflectance measurements were performed on dry and wet silver fir wood and were compared to Monte Carlo simulations, which consider the microstructure of the wood. An elementary model for the geometry of the wood's microstructure was assumed. The tracheids were described by long cylinders and all other scatterers were taken into account by an isotropic reduced scattering coefficient ($\mu_{s,iso}'$). In the theoretical model we applied the average diameter for the tracheids found in softwood. By using the refractive index of air, water and solid wood we calculated the scattering by the cylinders with an analytical solution of the

#93808 - $15.00 USD Received 13 Mar 2008; revised 28 Apr 2008; accepted 9 Jun 2008; published 20 Jul 2008

Maxwell equations. The only free parameter was $\mu'_{s,iso}$ both for the wet and dry wood. We changed $\mu'_{s,iso}$ until the difference between theory and experiments was minimal. We note that, by altering $\mu'_{s,iso}$ the reflectance perpendicular to the tracheids' direction ($R(x=0,y)$) stayed almost the same, only the reflectance parallel to the tracheids changed strongly. The smaller $\mu'_{s,iso}$ value which we found for wet wood as compared to dry wood can be explained by the smaller difference of the refractive index of water and wood substance as compared to the difference of n between air and wood substance. Thus, the reduced scattering coefficient due to the pitches and the rays, which both contribute to $\mu'_{s,iso}$, decrease. In addition, the surface scattering at the rough border between the lumen of the tracheids and the wood substance decreases when the difference of the refractive indices at the border decreases.

In general, we found that all features obtained in the spatially and time resolved experiments could be recovered by the theory. For example, we could explain the geometrical shapes of the iso-intensity contour lines of the spatially resolved reflectance measurements. Further, we could confirm the large difference of the reduced scattering coefficient of wet and dry wood. For wet wood the refractive index difference between the wood substance ($n=1.55$) and water ($n=1.33$) is much smaller than for dry wood ($n=1.0$). This implies that the reduced scattering coefficient of dry wood is much larger than for wet wood due to the smaller anisotropy factor of dry wood compared to that of wet wood. This is because the scattering coefficient μ_s is almost the same for dry and wet wood and $\mu'_s=\mu_s(1-g)$. In the simulations we found that μ'_s for dry wood compared to wet wood is about four times higher when determined perpendicular and more than two times higher when determined parallel to the tracheids. In the experiments the differences were even larger.

Quantitatively, differences both for spatially and time resolved reflectance data were found. In the time domain the determined reduced scattering coefficients exhibited differences up to 30% between Monte Carlo and time resolved experimental measurements. These differences can be considered as a good agreement when modeling a complex material such as wood that can show significant changes among different types of wood but also among trees of the same type. Further reasons for the differences between theory and experiments are: first, our model is relatively simple and can be further improved. For example, the traverse rays can be incorporated in the model. In addition, the change of the density of the tracheids in the early wood and in the late wood (they form together the growth rings) can be considered. Second, the refractive index of the wood substance is not well known. When using a different value for n of the wood substance all main characteristics of the remitted light will still be obtained, however, the quantitative values will change, and, thus, it might be possible to match also quantitatively the experimental data.

In literature similar measurements of the spatially resolved reflectance have been reported, however, completely different conclusions were made. For example, the authors argued that the scattering increased in wet wood as compared to dry wood [22].

In summary, we proposed a theoretical model based on the microstructure of softwood to simulate the light propagation in wood which is capable to describe all experimental features qualitatively. The model can be extended in several ways and can be used in different areas such as NIR spectroscopy of wood samples or computer graphics.

Acknowledgment

We acknowledge the support of the German Research Society (DFG).

#93808 - $15.00 USD Received 13 Mar 2008; revised 28 Apr 2008; accepted 9 Jun 2008; published 20 Jul 2008